

# Numerical modelling of road with chip seal surfacing layer

P. Kathirgamanathan, and P. R Herrington

*Opus International Consultants Ltd, Opus Research, 33 The Esplanade,*

*Petone, Lower Hutt 5012, New Zealand*

*padmanathan.kathirgamanathan@opus.co.nz*

**Abstract:** Most low-traffic roads are primarily thin chip seal surfacing with an unbound granular base and subgrades layers. This paper describes the development of a 3-D numerical model of a low-traffic road. The numerical model was built using the finite element modelling. A 3-D chip seal surface was constructed using X-ray tomography scans of multiple layer seal samples removed from a road. Stones particles were modelled as rigid body; the bitumen was modelled as deformable using a viscoelastic constitutive model. A stress dependent nonlinear anisotropic material model was used for the granular base and subgrade. The material parameters for the bitumen and granular layers are estimated using inverse modelling technique from experimental measurements. The inverse model is formulated as a non-linear least squares minimization problem coupled with a finite element model. It is done by constructing an iterative procedure using an optimisation routine in MATLAB's and at each iteration, finite element problem is solved.

**Keywords:** Finite element modelling; Inverse modelling; Parameter estimation; Chip seal surfacing, Pavement deformation;

## 1 Introduction

Chip seals surfacing provide low cost roads particularly in low traffic locations. Chip loss, cracks and permanent deformation of road layers reduces its strength and can result in traffic safety concerns. This problem may become more apparent with increasing axle loading and repetitions. Therefore, the assessment of the optimal cost and serviceability of a road design problem has to be studied carefully. This can be done efficiently by modelling the road response using numerical methods. The accuracy associated with modelling the road response is highly related to the material model used especially its material parameter values. Inaccuracy associated with model parameter values can lead

to differences between estimated and actual behaviour.

The numerical model of a road response simulation describes the mechanical response of a material under load. It could be used during the design process to study the effect of factors such as binder type, aggregate geometry and traffic stress on likely seal performance.

The novel concept of this paper is to demonstrate the work undertaken to construct a 3D chip seal surfacing road FEM using data derived from a real road surface and to exhibit methodologies for estimating material constants of bitumen and granular layers. In the present work the demonstration process is categorized into three parts. In the first part the construction of a 3-D finite element road model with a chip seal surfacing is considered. A 3-D chip layer was constructed using X-ray tomography scans of multiple layer seal samples removed from a highway. The preliminary development of this study is already reported in one of our previous paper [2]. In the second part the estimation of unknown parameters of bitumen using experimental data is demonstrated. It is based on dynamically loaded ball bearing assembly with the least square minimization technique and finite element modelling. In the third part the process for estimation of basecourse and subgrade layer parameters from falling weight deflectometer data is demonstrated. The inspiration behind the methodology is based on the work of [3].

## 2 Construction of finite element model of road

The geometry of the cross-section of an exemplary road cross-section can be seen in Figure 1. The geometry contains three layers, chip seal surface, base course, and subgrade. The chip seal layer contains stones and bitumen. Stones are assumed to be rigid body and bitumen was assumed to be viscoelastic. Both basecourse and subgrade are assumed to be deformable

with anisotropic material properties. The purpose of this section is to build a 3D finite element model similar to one given in Figure 1. The research strategy and methodologies are divided into three stages.

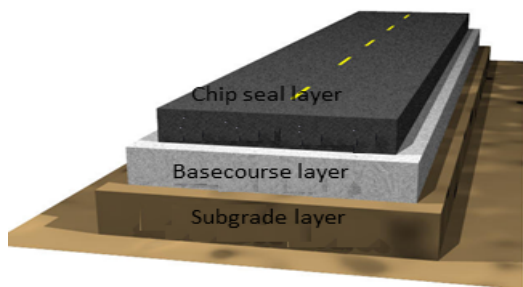


Figure 1: Road cross-section

In the first stage, the chip surfacing for the finite element model was built. It was done by recombining x-ray tomography cross sections of a real multiple layer chip seal core. This is arrived through several steps and based on the techniques available in literature for asphalt mix [4], [7].

1. Removed Seal sample from a highway as shown in Figure 2.



Figure 2: Original core

2. X-ray tomography scans of multiple layer seal samples were taken at 1.0 mm intervals and converted to grayscale images. Four of these images are shown in Figure 3.
3. A small section of the sample was selected to process as a 3D model. This was done in MATLAB by setting all pixels outside a certain domain as black.
4. The next step is to use the watershed function to try and segment the chip and then to create an image stack for each individual chip as shown in Figure 4.

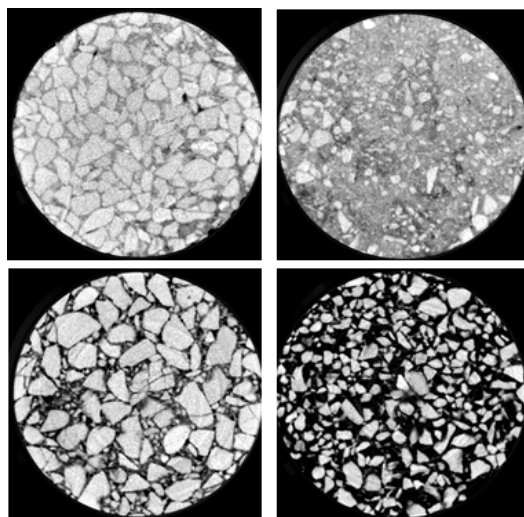


Figure 3: X-ray tomography scans

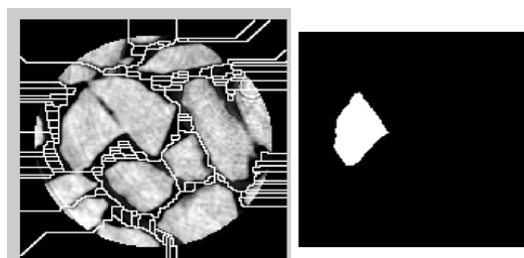


Figure 4: Result obtained from watershed transformed function

5. Once an image stack is prepared and ready to go, it can be transferred into an STL file as shown in Figure 5.

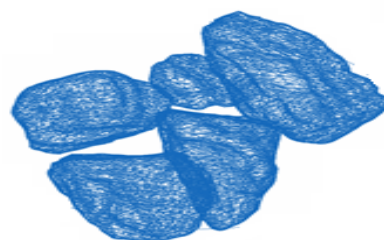


Figure 5: (A) Model chips and derived from X-ray tomography data

In the second step, the general purpose finite element program ABAQUS is used to build a complete model as shown in Figure 6. The model contains three layers. The dimension of the top chip seal layer is 60 mm × 80 mm × 10 mm. The bottom two layers are granular materials with 300 mm deep basecourse and

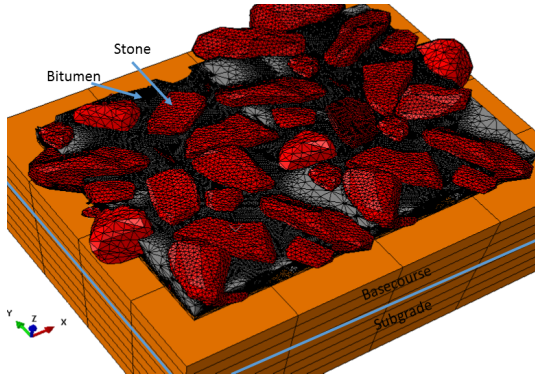


Figure 6: Finite element model

1000 mm deep subgrade materials. The chip was modeled as a rigid body. Bitumen properties were approximated using hyperelastic and viscoelastic material models. Hyperelasticity refers to materials which can experience large elastic strain that is recoverable. The deformation behaviour of these materials are often modelled by the Mooney–Rivlin model. The strain energy density function for an incompressible Mooney-Rivlin material is

$$W = C_1 (\bar{I}_1 - 3) + C_2 (\bar{I}_2 - 3) \quad (1)$$

where  $C_1$  and  $C_2$  are empirically determined material constants and  $\bar{I}_1$  and  $\bar{I}_2$  are the first and the second invariant of the deviatoric component of the left Cauchy-Green deformation tensor.

The stress function of a viscoelastic material is given in an integral form. Within the context of small strain theory, the constitutive equation for an isotropic viscoelastic material can be written as:

$$\sigma = \int_0^t 2G(t - \tau) \frac{de}{d\tau} d\tau + I \int_0^t 2K(t - \tau) \frac{d\Delta}{d\tau} d\tau \quad (2)$$

$$G(t) = G_\infty + \sum_{i=1}^{n_G} G_i \exp\left(-\frac{t}{\tau_i^G}\right)$$

$$K(t) = K_\infty + \sum_{i=1}^{n_K} K_i \exp\left(-\frac{t}{\tau_i^K}\right)$$

where  $\sigma$  Cauchy stress,  $e$  deviatoric part of the strain,  $\Delta$  volumetric part of the strain,  $t$  current time,  $\tau$  past time,  $I$  unit tensor,  $G_i$  shear elastic moduli,  $K_i$  bulk elastic moduli,  $\tau_i^G$ ,  $\tau_i^K$  are relaxation times for each component.

The bottom two layers are granular materials. Granular materials make up a discontinuous particulate medium physically and its resilient performance is strongly influenced by the applied wheel load. The resilient behaviour

of granular material is influenced by stress level, density, grain size, aggregate type, particle shape, moisture content, and number of load applications. There are several mathematical models have been developed using different stress components. One of the most popular model was developed by Uzan and is given by [6], [1]

$$M_r = k_1 P \left(\frac{\theta}{P}\right)^{k_2} \left(\frac{\tau_{oct}}{P} + 1\right)^{k_3} \quad (3)$$

where

$$\begin{aligned} \theta &= \sigma_1 + \sigma_2 + \sigma_3 \\ \tau_{oct} &= \frac{1}{3} \sqrt{(\sigma_1 - \sigma_2)^2 + (\sigma_2 - \sigma_3)^2 + (\sigma_3 - \sigma_1)^2} \\ P &= 100 \text{ kPa} \end{aligned}$$

$M_r$  resilient modulus,  $k_1$ ,  $k_2$ ,  $k_3$  are constants,  $\sigma_1$ ,  $\sigma_2$  and  $\sigma_3$  are principal stress.

The bottom boundary of the subgrade was fixed in all three directions. The side planes of the subgrade, basecourse and chip seal layers were free to move in all directions. The bitumen-chip, bitumen-basecourse and basecourse-subgrade interfaces were fixed (i.e. perfect adhesion).

The finite element model, which is capable of describing the behaviour of road deformation is built now. But several input data such as material constants are unknown. Laboratory and field experiments were conducted to estimate the constants appearing in the material models. The next two sections describes the equipment, trial procedure and estimation methodologies.

### 3 Experimental Measurements

#### 3.1 Steel sphere experiments

To determine the hyperelastic and viscoelastic parameters in the bitumen material model, experimental measurements were made using the apparatus shown in Figure 7. The 10 spheres (radius 25 mm) surrounding the central sphere were fixed. The central sphere was attached to the ram of a tensile testing machine and was lowered into position leaving a very small gap between it and the surrounding spheres. The assembly was filled with bitumen to a point half way up the top layer of spheres. The central sphere was then moved upwards and the subsequent force and displacement against time data recorded as shown in Figure 8. Tests were conducted at a loading rate of 0.4 kNs<sup>-1</sup>. The idea here was to provide a model of a stone particle



Figure 7: Steel ball assembly

in a seal layer with a wide range of bitumen film thicknesses.

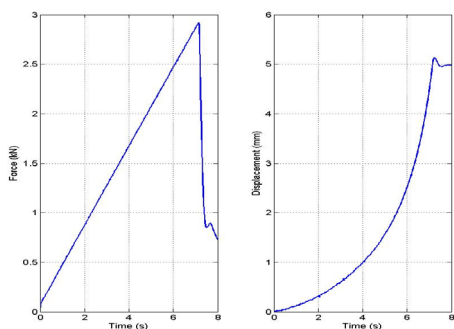


Figure 8: Force, displacement against time

### 3.2 FWD measurement

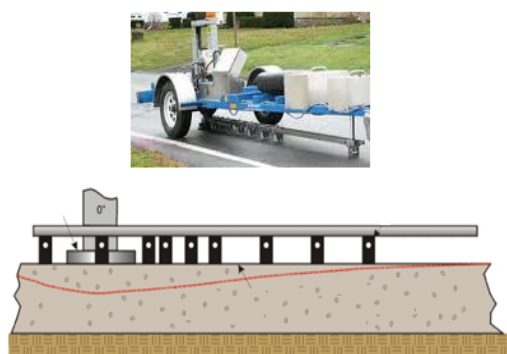


Figure 9: Falling weight deflectometer measurements

A falling weight deflectometer (FWD) is

Surface deflection	
Distance from center (mm)	Vertical displacement (mm)
0	1.062
200	0.738
450	0.282
600	0.165
900	0.079
1800	0.038

Table 1: Measured FWD deflection data

shown in Figure 9. It is a testing machine used by roading engineers to estimate the physical properties of road. The FWD is designed to impart a load pulse to the road surface. The FWD applies an impulsive load to the road surface and load is about  $566 \text{ kPa}$  upon a  $300 \text{ mm}$  diameter plate and a load impulse duration of  $25 \text{ ms}$ . The response of the road system is measured in terms of vertical deformation, or deflection, over a given area using geophones. The resulting vibration signal through the road is then received by a number of geophones set down linearly on the road in a particular pattern. Thus, the shape of deflection bowl is obtained. Table 1 shows the road deflection testing measurements for road surface comprised of basecourse and subgrade materials at offsets points  $0 \text{ mm}$ ,  $200 \text{ mm}$ ,  $450 \text{ mm}$ ,  $600 \text{ mm}$ ,  $900 \text{ mm}$ ,  $1800 \text{ mm}$  horizontally. This was measured under  $42 \text{ kN}$  load (equivalent to  $595 \text{ kPa}$ ).

## 4 Parameter estimation

The intention of parameter estimation procedure is the extraction of model constants from measured experimental data. It is a discipline, which offers tools for the competent use of data in estimation of constants appearing in the models. The measured values at certain observation points are the prime unknown in the forward problem. The material constants are unknown in the inverse problem. The aspiration here is to calculate the best estimates of these constants. This problem is known mathematically as an inverse problem and can be seen as an optimization problem whereby the objective function to minimize is the differences between the measured and the estimated values.

The first requirement in attempting to numerically calculate the material constants described above, is to be able to model accurately the forward problem, i.e. that of finding the stress, strain and deformation profile for a given set of material parameters and loading conditions.

### 4.1 Bitumen

In this section the finite element program has been used to simulate the same experiment described in section 3.1. The finite element model is shown in Figure 10 and its dimensions are: Diameter of sphere= 50 mm, Outside diameter of container 177 mm, wall thickness 25 mm and wall height=110 mm. The steel spheres are assumed to be rigid and made of H13 steel. No rotation or translation were permitted on spheres inside the bitumen and the top sphere was allowed to move on the vertical directions. The bottom of the container was constrained for all degrees of freedom. Perfect adhesion between the spheres and bitumen is assumed. The top sphere was pulled upwards with 0.4 kN/s and the displacement changes against time was calculated.

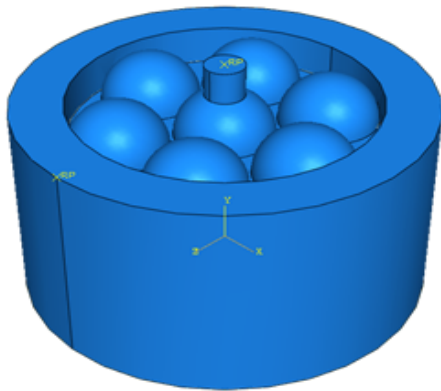


Figure 10: FEM model of ball bearings

The calculation process begins by assuming randomly chosen initial values for the constants appearing in the hyper elastic and viscoelastic models. It is an iterative process, and improved the original estimates are by minimizing the sum of the square of the differences between experimental values and the corresponding FEM calculated result i.e. minimising the function  $f(\mathbf{p})$ :

$$f(\mathbf{p}) = \sqrt{\frac{1}{n} \sum_{k=0}^n \left( \frac{d_i^{FEM}(\mathbf{p}) - d_i^{exp}}{d_i^{exp}} \right)^2} \quad (4)$$

where  $\mathbf{p}$  is the vector of constants to be estimated,  $n$  is the number of experimental values,  $d_i^{exp}$  is the  $i$ -th experimental value and  $d_i^{FEM}$  is the  $i$ -th FEM value. For the optimal fit  $\mathbf{p}$  must be varied to minimise  $f$ .

The whole model is built in MATLAB platform. A PYTHON program is used to communicate between MATLAB and finite element

program Abaqus. The minimization process is implemented using MATLABs *lsqnonlin* function which uses the Levenberg-Marquardt algorithm.

The non-linear objective function given above may have more than one minimum. Therefore, the solution process should include finding the global minimum. To deal with these problems, first all or most of the local minima of objective function at a larger interval were estimated. Then the lowest value of the minima was picked. In the next step the minimum obtained from the previous step was used as the starting value to solve the problem.

### 4.2 Basecourse and Subgrade

In this section the finite element program has been used to set up the forward model described in section 3.2 in three dimensions. To reduce the computational effort by making use of the symmetry in the geometry and loading only the quarter of the model is considered as shown in Figure 11. The dimension of FEM model is 2 m × 1.5 m × 1.3 m. The bottom of the model was constrained for all degrees of freedom. Lateral displacements  $u_x$  and  $u_y$  are restrained in X and Y directions, respectively, along the vertical planes ( $u_x, u_y = 0$ ). The model contains two layers and assumed to be a deformable with anisotropic material properties. The basecourse and subgrade layers are 300 mm, 1000 mm height respectively and their material properties are modelled by equation 3.

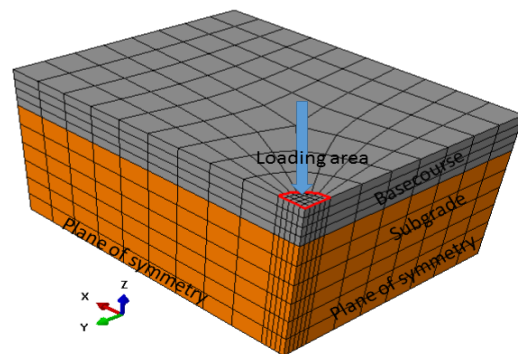


Figure 11: FEM model of basecourse and subgrade

Similar to the procedure described in section 4.1, the modelling procedure of the forward problem was started by randomly chosen material parameter values of Equation 3 and then the deflection at points 0, 200, 300, 450, 600, 900 and 1800 mm were compared with their re-

spective measured values. This procedure was repeated by changing material constants until the differences between the measured and simulated deflection data are very small as in section 4.1.

### 5 Results and Discussion

In this section, numerical calculations are presented to demonstrate the modelling process and evaluate the accuracy of the model predictions. To do so, the experimental data obtained from the experiment described in section 3.1 and 3.2 for two different loading conditions are considered and compared with the model predictions.

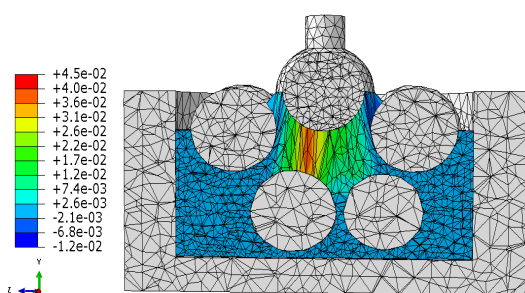


Figure 12: Cross-sectional view of FEM-Vertical strain

Figure 12 shows the cross-sectional view of vertical stress contours when the simulation has been continued sufficiently for some time. Figure 13A shows the displacement-time experimental data at a loading rate of  $0.4 \text{ kNs}^{-1}$  used to fit the model constants in Equation 4 along with the resulting simulation. The procedure produced good agreement between measured and predicted data. The derived model constants were also validated by simulating experiments at different loading rates and comparing to experimental data. Figure 13B compares simulation results to experimental data at a loading rate of  $0.8 \text{ kNs}^{-1}$ .

Figure 14 shows the contour plot of vertical displacement under a FWD load impulse. Figure 15 shows the FWD data used to fit the model constants in Equation 5 along with resulting vertical surface deflection of road FEM. The procedure produced good agreement between measured and estimated data. The derived model constants were also validated by simulating experiments at different FWD loading cases and comparing to measured data. Finally a number of simulations were run to examine the effect of loading in the chip seal layer.

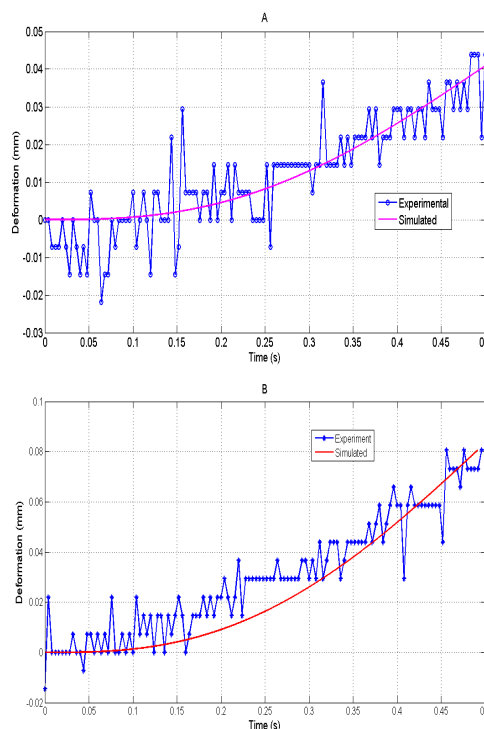


Figure 13: (A) Comparison of experimental values used for parameter fitting and the resulting simulation, (B) Comparison of experimental values with simulation results at a different loading rate.

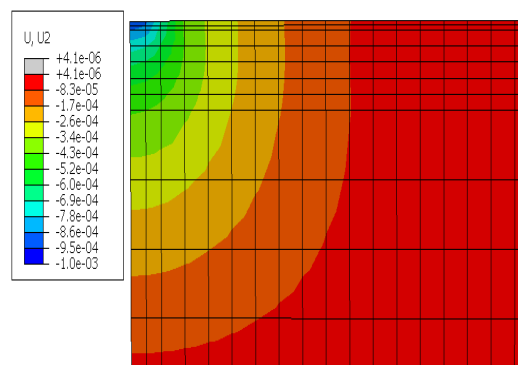


Figure 14: Contour plot of vertical deflection.

One such case is shown in Figure 16, which is the contour plot of horizontal strain when a load was applied. The effect of chip size, embedment depth, variations in the chip seal layer height, variations in loading magnitude and directions on the model predictions will be studied and reported in our future publications.

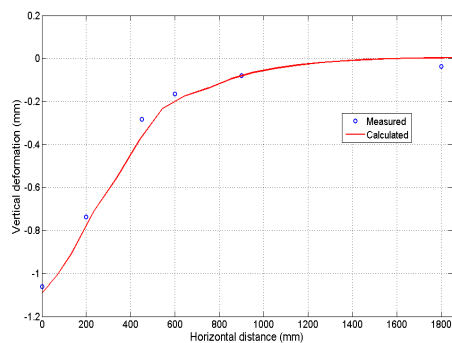


Figure 15: Calculated and measured strain values.

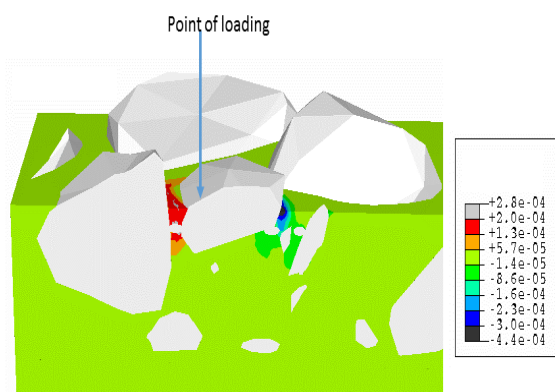


Figure 16: Cross section showing horizontal strains. Tensile strains are positive.

## 6 Summary and Conclusion

The intention of this paper is to demonstrate development of a 3D finite element model of a low traffic road. The development process is classified into three parts: (a) building a fem model and (b) estimation of material constants of bitumen, (c) estimation of material constants of basecourse and subgrade. The use of x-ray tomography of a real chip seal core was used in construction of a surface layer of finite element model and a stress dependent nonlinear anisotropic material model was used for the granular base and subgrade.

The material parameter estimation is based on a nonlinear least squares coupled with finite element techniques. Nonlinear least squares minimization is done by constructing an iterative procedure using MATLAB's inbuilt function *lsqnonlin* and at each iteration, finite element solutions to the deformation are solved using the ABAQUS Finite element program.

An examples given in section 5 demonstrates

how the model is able to determine the constants appearing in the model and predict the deformation behaviour. The results from these examples suggest that the inverse model described above is capable of estimating the constants to a reasonable degree of accuracy.

## References

- [1] Bruce S., The development and verification of a pavement response and performance model for unbound granular pavements, *PhD Thesis, University of canterbury*, 2005.
- [2] Kathirgamanathan, P., Herrington P. R., and McIver, I., Chip Seal Finite Element Model, *Seventh International Conference on Maintenance and Rehabilitation of Pavements and Technological Control*, 2012.
- [3] Kathirgamanathan, P., Neitzert T., Optimal Process Control Parameters Estimation in Aluminium Extrusion for Given Product Characteristics, *Proceedings of the World Congress on Engineering*, vol II, 2008, 1436–1441.
- [4] Kutay, M. E., Arambula, E., Gibson, N., & Youtcheff, J., Three-dimensional image process methods to identify and characterize aggregates in compacted asphalt mixtures, *International Journal of Pavement Engineering* 11(6): 511-528, 2010.
- [5] Uzan, J., Characterization of Granular Material, *Transportation Research Record*, 1022, 52–59.
- [6] Werkmeister S., Permanent Deformation Behaviour of Unbound Granular Materials in Pavement Constructions, *PhD thesis, Dresden University*, 2003.
- [7] Zelelew, H. M., & Papagiannakis, A.T., A volumetrics thresholding algorithm for process asphalt concrete X-ray CT images, *International Journal of Pavement Engineering* 12(6): 543-551, 2011.